Phase Stability and Defect Physics of a Ternary $ZnSnN_2$ Semiconductor: First Principles Insights

Shiyou Chen, Prineha Narang, Harry A. Atwater,* and Lin-Wang Wang**

Direct bandgap, earth abundant semiconductors with E_g around 1.5 eV are essential for both photovoltaic and solar to fuel (photocatalytic) energy conversion.[1,2] Among the conventional semiconductors, such as element Si and Ge, binary III-V (III = B, Al, Ga, In; V = N, P, As, Sb) and II-VI (II = Zn, Cd; VI = O, S, Se, Te), only a limited number of candidates have suitable bandgaps in the range 1.0–2.0 eV.[3] This motivates the search for earth-abundant alternatives to current semiconductors for efficient, high-quality optoelectronic devices, photovoltaics and photocatalytic energy conversion.[4] One methodology for the search is to study ternary and multi-ternary semiconductors with more elements and more flexible optoelectronic properties.

Fifty years ago, the design of ternary and quaternary semiconductors through the cation mutation in binary II-VI and III-V semiconductors was proposed by Goodman and Pamplin:[5–7] (i) Through replacing two Zn atoms in ZnSe by one Cu and one In atom, ZnSe is mutated into ternary $CuInSe_2$, and if further replacing two In by Zn and Sn, $CuInSe_2$ is mutated into quaternary $Cu_2ZnSnSe_4$. Both $CuInSe_2$ and $Cu_2ZnSnSe_4$ are high-efficiency light-absorber semiconductors for thin film solar cells, which have been under intensive study during the past 30 years.[8–10] (ii) Similarly through replacing two Ga in GaN by Zn and Sn, GaN can be mutated into $ZnSnN_2$, as shown in **Figure 1**. In fact this cation mutation, a cross substitution, leads to a class of ternary II-IV-V_2 semiconductors with II = Zn, Cd, IV = Si, Ge, Sn and V = N, P, As, Sb, e.g., $ZnGeN_2$ and $ZnSnP_2$. II-IV-N_2 compounds are closely related to the wurtzite-structure III-N semiconductors, but have a mixed A-site composition. The choice of different group II and group IV elements provides chemical diversity that can be exploited to tune structural and electronic properties through the series.

Compared to the well-studied $CuInSe_2$ (I-III-VI_2 class), the II-IV-V_2 semiconductors have not been studied extensively, e.g., the crystal structures and bandgaps of some II-IV-V_2 have been determined until quite recently.[12,13] One possible reason for the slow progress in the study of II-IV-V_2 materials may be related to the difficulty in synthesis of electronic quality samples.[14,15] With additional elements, it is more challenging to control the composition and to synthesize single-phase and stoichiometric ternary compounds. Using RF magnetron sputter deposition, our group recently synthesized a new II-IV-V_2 compound, $ZnSnN_2$, for which the optical measurements reveal a direct bandgap about 2.0 eV.[16] Using different methods, Feldberg et al.[17,18] and Quayle et al.[19] have also synthesized $ZnSnN_2$ samples recently. The successful synthesis of $ZnSnN_2$ indicates that a series of II-IV-V_2 semiconductors may be synthesized in the future and a rich space of the material properties may be explored for different functionalities.

An unusual feature of the synthesized $ZnSnN_2$ samples is the high concentration of electron carriers (10^{19} to 10^{21} cm^{-3}, almost metallic) according to Hall measurements,[16,18] which can change the onset of the light absorption spectrum due to the Burstein-Moss effect.[16,18] However, the origin of the very high concentration of electrons is not evident, and therefore it is not clear whether the high electron concentration comes from the coexistence of elemental metal phases, or the formation of intrinsic defects. In this communication, we use the first-principles calculations to study the phase stability and defect properties of $ZnSnN_2$, in order to reveal the origin of the high electron concentration.

Phase Stability: At the ground state, $ZnSnN_2$ crystalizes in a structure in the $Pna2_1$ symmetry with a 16-atom primitive cell,[12,16] as shown in Figure 1b. To study its thermodynamic stability, we first calculated its formation energy (enthalpy), $\Delta H_f(ZnSnN_2)$, which is defined as the total energy change of the following reaction,

$$\mathrm{Zn(hcp) + Sn(diamond) + N_2(gas) \rightarrow ZnSnN_2} \quad (1)$$

where Zn is in the hexagonal-close-packed (HCP) structure, Sn is in the diamond structure and N_2 is at the gas molecule state. Using the hybrid functional with $\alpha = 0.31$ (see the Computational Section for details), a very small $\Delta H_f(ZnSnN_2) = -0.17$ eV/f.u. is found (the value is –0.13 eV/f.u. if $\alpha = 0.25$). Since the calculated formation energy of compound semiconductors are sensitive to the specific pseudopotentials and functionals,[20,21] we also used a recently developed scheme by Stevanović et al. which can predict the formation energy of compound semiconductors with a high accuracy (the test calculations on 55 ternary compounds show that the mean absolute error is only 0.048 eV/atom),[21] in order to evaluate the influence of the calculation methods. The calculation details of the new scheme is given in Ref. [21]. Using the new scheme,

S. Chen, P. Narang, H. A. Atwater, L.-W. Wang
Joint Center for Artificial Photosynthesis, CA, USA
E-mail: cshiyou@gmail.com; haa@caltech.edu; lwwang@lbl.gov
S. Chen, L.-W. Wang
Materials Sciences Division
Lawrence Berkeley National Laboratory
One Cyclotron Road
Mail Stop 66, Berkeley, CA 94720, USA
P. Narang, H. A. Atwater
Thomas J. Watson Laboratories of Applied Physics
California Institute of Technology Pasadena, CA 91125, USA

DOI: 10.1002/adma.201302727

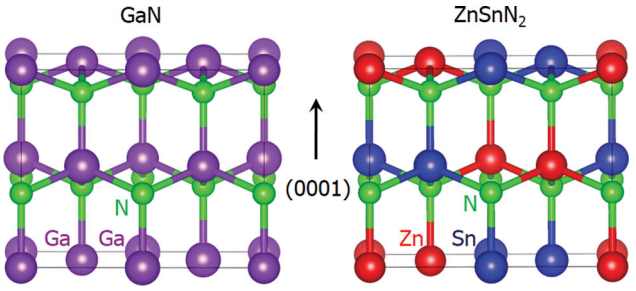

Figure 1. The crystal structure plot of wurtzite GaN and $ZnSnN_2$. Here GaN is plotted in a supercell with the same size as the primitive cell of $ZnSnN_2$ in the $Pna2_1$ symmetry. The $Pna2_1$ structure of $ZnSnN_2$ is equivalent to the wurtzite-kesterite I_2-II-IV-VI_4 structure through replacing I by Zn, II and IV by Sn, and VI by N.[11]

$\Delta H_f(ZnSnN_2) = -0.14$ eV/f.u., in good agreement with the value from the hybrid functional calculation. To compare with the experimental values, similar calculations are performed for other compounds, $\Delta H_f(Zn_3N_2) = -0.33$ eV/f.u. (experimental: –0.25 eV/f.u.),[21] $\Delta H_f(GaN) = -1.43$ eV/f.u. (experimental: –1.62 eV/f.u.).[21] Considering the small error with the new scheme, we believe the small formation energy of $ZnSnN_2$ has a high reliability. We notice that a large $\Delta H_f(ZnSnN_2) = -2.32$ eV/f.u. had been reported from the calculation using the linearized gradient muffin-tin orbital (LMTO) method,[22] which is in contrast with the present results using the plane-wave pseudopotential method and the new scheme, and the origin of the inconsistence is so far not clear.

Now we will discuss how the small formation energy influences the synthesis of $ZnSnN_2$. In the synthesis environment, the "richness" or partial pressure of the component elements can be tuned, which can be quantitatively described by the chemical potentials of the component elements, μ_{Zn}, μ_{Sn} and μ_N. $\mu_{Zn} = 0; \mu_{Sn} = 0; \mu_N = 0$ are defined when Zn, Sn and N are so rich that their pure elemental phase like HCP Zn, diamond Sn, N_2 molecule can be formed. To avoid the formation of secondary phase such as the elemental phases and binary compound Zn_3N_2, the following conditions should be satisfied,

$$\begin{aligned} &\mu_{Zn} < 0; \mu_{Sn} < 0; \mu_N < 0 \\ &3\mu_{Zn} + 2\mu_N < \Delta H_f(Zn_3N_2) \end{aligned} \quad (2)$$

Under the thermodynamic equilibrium state that stabilizes $ZnSnN_2$, the following equation should also be satisfied,

$$\mu_{Zn} + \mu_{Sn} + 2\mu_N = \Delta H_f(ZnSnN_2) \quad (3)$$

With all these requirements satisfied, μ_{Zn} and μ_{Sn} are limited in a certain region in the (μ_{Zn}, μ_{Sn}) plane as shown in **Figure 2**a, and μ_N depends on them according to Equation (3). As a result of the small $\Delta H_f(ZnSnN_2)$, the stable region of $ZnSnN_2$ is quite narrow, and the tunable range of μ_{Zn} and μ_{Sn} is less than 0.05 eV. In contrast, another closely related II-IV-V_2 semiconductor $ZnGeN_2$ has a much larger formation energy (–1.31 eV/f.u.) and wider stable region in the (μ_{Zn}, μ_{Ge}) plane, as shown in Figure 2b. The obvious difference indicates that it is much more difficult to synthesize single-phase $ZnSnN_2$ than $ZnGeN_2$. Actually in the literature, $ZnGeN_2$ had been synthesized for decades[14,15,23,24] while $ZnSnN_2$ had only be synthesized recently.[16–19] The reason for the large difference may be related to the weaker Sn-N bond than Ge-N, which also causes the Sn-N compound Sn_3N_4 to have a positive formation energy (so not shown in Figure 2, the experimental value is still unavailable)[25,26] while Ge_3N_4 have a negative formation energy –0.98 eV/f.u. The much smaller formation energy of $ZnSnN_2$ than that of $ZnGeN_2$ is comparable with the situation between InN (–0.06 eV/f.u.) and GaN (–1.43 eV/f.u.).[21] As a result of narrow small stable region, the coexistence of secondary phases such as Zn, Sn metals and Zn_3N_2 is highly possible in the synthesized samples. The coexisting Zn or Sn metal can be one possible origin of the high electron concentration. Based on these results, strategies to avoid the formation and exclude the coexistence of these secondary phases are critical to future applications and improvement of the $ZnSnN_2$ semiconductor.

Defect Physics: Alternative to the formation of secondary phases, the formation of point defects in the $ZnSnN_2$ lattice is also possible, and influences its properties. Whether a point defect α in the charge state q will form or not depends on its formation energy, $\Delta H(\alpha, q)$, which is a function of the chemical potential of elements and chemical potential of electrons (Fermi energy), as described by,

$$\Delta H(\alpha, q) = \Delta H_0(\alpha, q) + \sum_i n_i \mu_i + q E_F \quad (4)$$

where $\Delta H_0(\alpha, q)$ is the formation energy when the chemical potentials μ_i of all elements i (i = Zn, Sn, N) are zero and the Fermi energy $E_F = 0$ (E_F is referenced to the valence band maximum (VBM) eigenenergy of the host semiconductor), and can be calculated using the supercell model.[27,28] n_i is the number of atom i, and q is the number of electrons exchanged between the semiconductor and the atmosphere in forming the defect.

The calculated formation energies of six possible defects in $ZnSnN_2$ is shown in Figure 2c, where the lowest-energy charge state is shown for each defect at a certain Fermi energy and the chemical potentials of the elements are set at the center of the stable region in Figure 2a. Two obvious characters can be identified: (i) the donor defects such as Sn_{Zn} antisite (Sn substituting Zn), V_N (N vacancy) and Zn_i (Zn on the interstitial site surrounded by four N anions) have much lower formation energy than the acceptor defects, such as Zn_{Sn}, V_{Zn} and N_i. The much lower formation energies of these donor defects determine the intrinsic n-type conductivity (self-doping) of $ZnSnN_2$. The values become negative when the Fermi energy approaches zero (VBM), i.e., they will form spontaneously in p-type samples, quenching mobile hole conductivity and pinning the Fermi energy close to the conduction band minimum (CBM) energy, so the p-type doping is impossible based on this thermodynamic analysis. This can also be understood according to the low VBM energy of $ZnSnN_2$ (the GaN/$ZnSnN_2$ valence band offset calculation shows that the VBM of $ZnSnN_2$ is as low as that of GaN)[29] and the conventional doping limit rule, which states that a semiconductor is difficult to be doped p-type if the valence band is too low in energy.[30]

(ii) Sn_{Zn} antisite has the lowest formation energy through the whole Fermi energy range, so it is the dominant intrinsic

Adv. Mater. **2013**,
DOI: 10.1002/adma.201302727

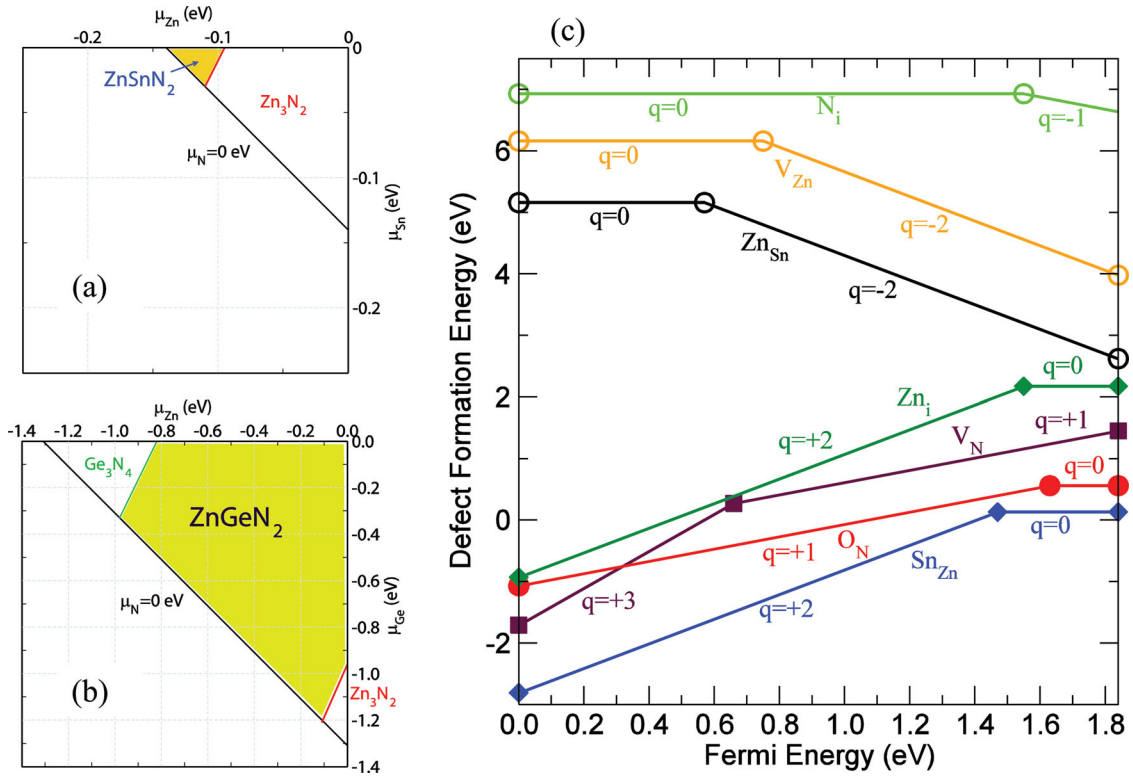

Figure 2. (a) and (b) The calculated chemical potential regions (in yellow shadow) that stabilize single-phase $ZnSnN_2$ (a) and $ZnGeN_2$ (b). Outside the yellow region, different secondary phases as labeled will form. (c) The change of the defect formation energy as a function of the Fermi energy when $\mu_{Zn} = -0.11$ eV, $\mu_{Sn} = -0.02$ eV, $\mu_N = -0.02$ eV. The slope of the change shows the charge state q, and only the most stable charge state is plotted for a certain Fermi energy. The turning points show the transition energy levels at which the charge states change.

defect of this ternary semiconductor. At the neutral charge state (q = 0), the formation energy is only 0.13 eV, which corresponds to a population around 10^{20} cm^{-3} at the room temperature, and an even higher population at higher growth temperature. As a donor defect, Sn_{Zn} induces a donor level below the CBM state, which are occupied by two electrons (Sn has two more valence electrons than Zn). The calculated (0/2+) transition energy level of Sn_{Zn} is 0.37 eV below CBM, i.e., when the Fermi energy is below this level, Sn_{Zn} will be ionized and the two electrons on the donor level will be donated to the system. Since it has a much lower formation energy and thus much higher population than any other intrinsic defects, the Fermi energy of the $ZnSnN_2$ samples is pinned by Sn_{Zn} to above the (0/2+) transition energy level.

Although the transition energy level of Sn_{Zn} is not shallow, the corresponding donor state is not localized, as shown by the delocalized wave-function over the whole supercell in **Figure 3**c. This can be understood according to its component. The bandgap of $ZnSnN_2$ is opened between the valence band states composed of N-2p+Zn-3d orbitals and the conduction band states composed of Sn-5s+N-2s orbitals (see Figure 3a).[29] The donor state of Sn_{Zn} has the similar component to the lowest conduction band states, and is distributed on all Sn and N atoms in the whole supercell. Considering that the concentration of the neutral Sn_{Zn} can be as high as 10^{20} cm^{-3} (one defect among hundreds of atoms), the interaction between the nearby defects makes the donor states be continuous to form an occupied defect band, as shown schematically in Figure 3a. Our calculation with one Sn_{Zn} defect in an 128-atom supercell and $2 \times 2 \times 2$ k-point mesh shows that the Sn_{Zn} defect band has a large dispersion (2 eV band width) and overlaps with the conduction bands. Because of the overlapping, the electrons in this defect band can be taken as the electron carriers (Note, this is insensitive to the calculated (0/2+) level, and different from the situation when the defect concentration is low and the electrons on the donor states need to be ionized to the conduction band to become the electron carriers) and the system becomes almost metallic, which gives an explanation to the high concentration of electron carriers revealed by the Hall measurement.[16,18] Since the tunable chemical potential range of Zn and Sn is very narrow (less than 0.05 eV), it is limited to increase the Sn_{Zn} formation energy by changing the chemical potential of elements, and thus it is difficult to suppress the electron concentration in $ZnSnN_2$ by changing the growth environment.

With the possible origin of the high electron concentration attributed to high population of Sn_{Zn} defects, we need to revisit the Burstein-Moss effect in $ZnSnN_2$ samples,[16,18] which means that when the free electrons fill the conduction bands, the absorption onset shifts to higher energy. However, in $ZnSnN_2$ the electrons are actually occupying the donor defect bands below the CBM rather than filling the conduction band, as shown schematically in Figure 3a, so the absorption onset

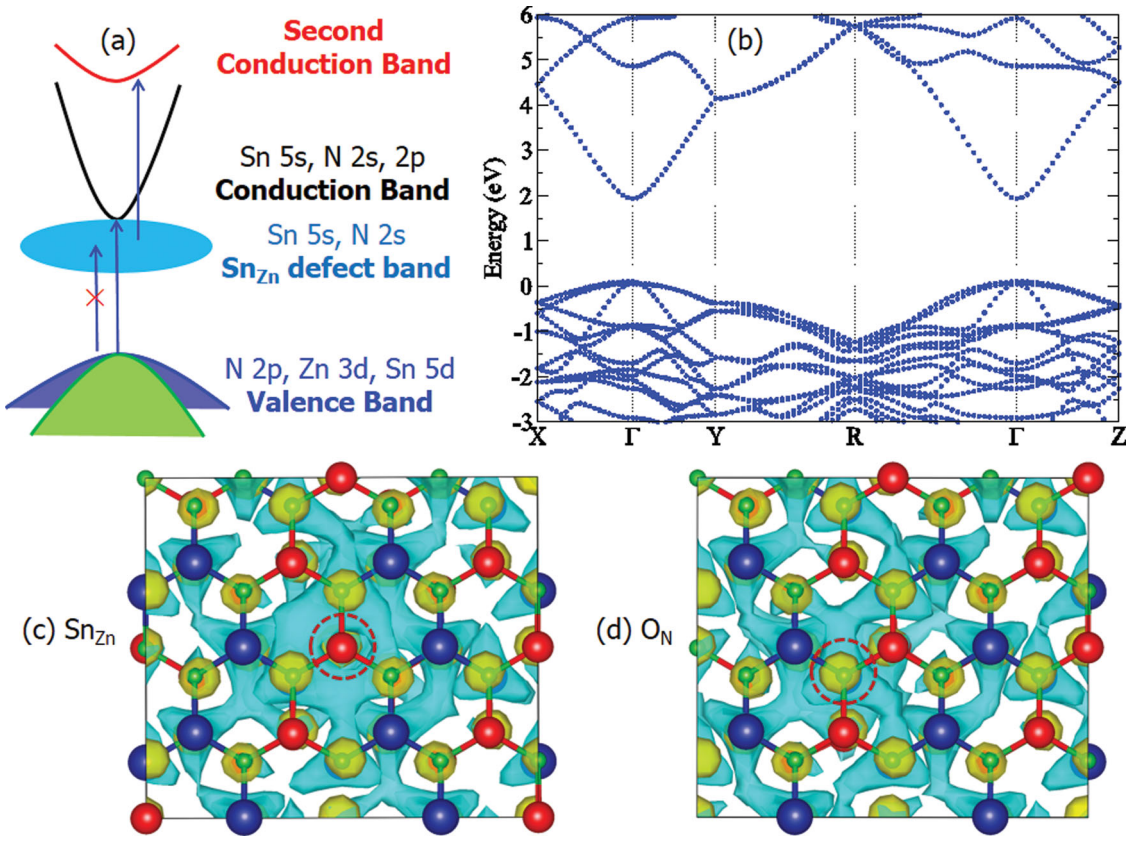

Figure 3. (a) Schematic plot of $ZnSnN_2$ band structure, with the Sn_{Zn} defect band below the lowest conduction band. (b) Calculated band structure of $ZnSnN_2$ along high-symmetry lines in the Brillouin zone. (c) the wavefunction of Sn_{Zn} donor state, (d) the wavefunction of O_N donor state. For (c) and (d), the defect and dopant concentration is 5.6×10^{20} cm^{-3}.

of photons will not shift up significantly with the electron concentration, i.e., the high electron concentration produced by the Sn_{Zn} defects in $ZnSnN_2$ does not result in obvious Burstein-Moss effect. On the other hand, possible absorption may also happen through the electron excitation from the occupied defect band to the higher energy conduction band. However, both our calculated band structure (Figure 3b) and previously calculated band structure using different functionals show that the second conduction band is more than 2.5 eV higher than the lowest conduction band,[12,16] so there is no direct absorption of lower-energy photons. Based on this analysis, the bandgap (about 2.0 eV) revealed by optical measurements[16] should be close to the fundamental bandgap of the defect-free $ZnSnN_2$. Because of the coexistence of metal-like high electron concentration and the 2.0 eV absorption onset (bandgap), $ZnSnN_2$ can be taken as a new conducting material, which has a narrower bandgap than the conventional wide-gap transparent conducting oxides.[31,32]

In addition to the intrinsic defects, unintentional doping by extrinsic impurity atoms is also possible, e.g., the O impurity atom may exist in the lattice. The calculated formation energy of O_N is shown in Figure 2c when the oxygen chemical potential $\mu_O = \Delta H_f(ZnO) - \mu_{Zn} = -3.43$eV, and the value can be decreased significantly as μ_O increases (the oxygen partial pressure increases). Therefore, a very low partial pressure of oxygen is required to suppress the formation of O_N antisites,[33] otherwise, O_N donors can also cause a high electron concentration. The (0/+) transition energy level of O_N is 0.21 eV below CBM and the corresponding donor state is also delocalized over the whole supercell, as shown in Figure 3d, so the O_N states can also form a defect band, similar to the Sn_{Zn} states. Therefore the above discussion about the donor defect band and optical transitions work also for the O_N impurities.

In conclusion, we find that $ZnSnN_2$ has a very small formation enthalpy and a narrow stable region in the element chemical potential space, so its single-phase synthesis is a challenge. The study of defect properties shows that the semiconductor is intrinsically self-doped to n-type by high population of defects such as the dominant Sn_{Zn} antisites and the possible O_N impurities. The high population of these donor defects results in a high concentration of electron carriers, and makes the system almost metallic (degenerately n-type), explaining the experimental observation. Since these electrons stay on the donor defect band below the CBM, they do not influence the onset of the optical absorption (optical bandgap) significantly. Therefore $ZnSnN_2$ can be regarded as a new material that combines a metallic conductivity with a direct semiconductor bandgap.

Computational Section

The structural relaxation and electronic structure calculations are performed within the density functional theory (DFT)

Adv. Mater. **2013**,
DOI: 10.1002/adma.201302727

formalism as implemented in the VASP code.[34] The frozen-core projector augmented-wave potentials[35] are employed with an energy cutoff of 400 eV for the plane wave basis set. A 6 × 6 × 6 Monkhorst-Pack k-point mesh is included in the Brillouin zone integration for the 16-atom primitive cell and single k-point is included for the 128-atom supercell, which is used for the simulation of defects. Test calculations with denser k-point mesh show the calculated results are well converged. The image charge correction was not included in the present calculation, because the donor defects (such as Sn_{Zn}) that we are interested in have quite delocalized donor states, as shown in Figure 3. According to the previous work by Wei, if the defect state is delocalized (not like point charge), the image charge effect is not significant and the Makov-Payne correction tends to overestimate this effect for defects with delocalized states.[27] For the exchange-correlation functional, we use the non-local hybrid functional (HSE)[36] in which a percentage (known as the mixing parameter α) of the semi-local GGA exchange potential is replaced by screened Fock exchange. Here based on the similarity in the crystal and electronic structure between GaN and $ZnSnN_2$, the mixing parameter α is set to 0.31, following the previous calculation setup which predicts a bandgap of 3.5 eV for GaN, in good agreement with the experimental value.[37,38] It predicts the lattice constants a = 6.70, b = 5.81, c = 5.42 Å (close to the experimental values)[16,18] and a direct bandgap of 1.84 eV for $ZnSnN_2$, close to the value from the optical measurement (2.0 eV).[16] We notice that there are contradictive results in the calculated bandgaps from different level of approximations to the exchange-correlation functional, from 1.42 eV (HSE with $\alpha = 0.25$)[16] to 2.02 eV (GW).[12,22] To see if such approximations influence the conclusions of the current paper, test calculations are also performed with different α parameters ($\alpha = 0, 0.25$), which show that the conclusions are independent of the specific functionals.

Acknowledgements

This material is based upon work performed by the Joint Center for Artificial Photosynthesis, a DOE Energy Innovation Hub, supported through the Office of Science of the U.S. Department of Energy under Award Number DE-SC0004993. Prineha Narang is supported by the National Science Foundation Graduate Research Fellowship and the Resnick Sustainability Institute.

Received: June 14, 2013
Revised: July 24, 2013
Published online:

[1] W. Shockley, H. J. Queisser, *J. Appl. Phys.* **1961**, *32*, 510.
[2] M. Grätzel, *Nature* **2001**, *414*, 338.
[3] O. M. Madelung, *Semiconductors: Data Handbook*, Springer, Berlin, **2004**.
[4] S. Curtarolo, G. L. W. Hart, M. B. Nardelli, N. Mingo, S. Sanvito, O. Levy, *Nature Mater.* **2013**, *12*, 191.
[5] C. H. L. Goodman, *J. Phys. Chem. Solids* **1958**, *6*, 305.
[6] B. R. Pamplin, *J. Phys. Chem. Solids* **1964**, *25*, 675.
[7] S. Chen, X. G. Gong, A. Walsh, S.-H. Wei, *Phys. Rev. B* **2009**, *79*, 165211.
[8] J.-F. Guillemoles, U. Rau, L. Kronik, H.-W. Schock, D. Cahen, *Adv. Mater.* **1999**, *11*, 957.
[9] S. Chen, X. G. Gong, A. Walsh, S.-H. Wei, *Appl. Phys. Lett.* **2009**, *94*, 041903.
[10] S. B. Zhang, S.-H. Wei, A. Zunger, H. Katayama-Yoshida, *Phys. Rev. B* **1998**, *57*, 9642.
[11] S. Chen, A. Walsh, Y. Luo, J.-H. Yang, X. G. Gong, S.-H. Wei, *Phys. Rev. B* **2010**, *82*, 195203.
[12] A. Punya, W. R. L. Lambrecht, M. van Schilfgaarde, *Phys. Rev. B* **2011**, *84*, 165204.
[13] D. O. Scanlon, A. Walsh, *Appl. Phys. Lett.* **2012**, *100*, 251911.
[14] J. Muth, A. Cai, A. Osinsky, H. Everitt, B. Cook, I. Avrutsky, *MRS Syposium Proceedings* **2005**, *831*, 745.
[15] J. Nostrand, J. Albrecht, R. Cortez, K. Leedy, B. Johnson, M. Okeefe, *Journal of Electronic Materials* **2005**, *34*, 1349.
[16] L. Lahourcade, N. C. Coronel, K. T. Delaney, S. K. Shukla, N. A. Spaldin, H. A. Atwater, *Adv. Mater.* **2013**, *25*, 2562.
[17] N. Feldberg, B. Keen, J. D. Aldous, D. O. Scanlon, P. A. Stampe, R. J. Kennedy, R. J. Reeves, T. D. Veal, S. M. Durbin, *2012 38th IEEE Photovoltaic Specialists Conference (PVSC)* (**2012**), p. 2524.
[18] N. Feldberg, J. D. Aldous, W. M. Linhart, L. J. Phillips, K. Durose, P. A. Stampe, R. J. Kennedy, D. O. Scanlon, G. Vardar, R. L. Field, T. Y. Jen, R. S. Goldman, T. D. Veal, S. M. Durbin, *Appl. Phys. Lett.* **2013**, *103*, 042109.
[19] P. C. Quayle, K. He, J. Shan, K. Kash, *MRS Communications* **2013**, FirstView, 1.
[20] M. Fuchs, J. L. F. Da Silva, C. Stampfl, J. Neugebauer, M. Scheffler, *Phys. Rev. B* **2002**, *65*, 245212.
[21] V. Stevanović, S. Lany, X. Zhang, A. Zunger, *Phys. Rev. B* **2012**, *85*, 115104.
[22] A. Punya, T. R. Paudel, W. R. L. Lambrecht, *Physica Status Solidi (c)* **2011**, *8*, 2492.
[23] J. L. Shay, E. Buehler, J. H. Wernick, *Phys. Rev. B* **1971**, *3*, 2004.
[24] K. Du, C. Bekele, C. Hayman, J. Angus, P. Pirouz, K. Kash, *Journal of Crystal Growth* **2008**, *310*, 1057.
[25] R. Mientus, K. Ellmer, *Surface and Coatings Technology* **1999**, *116*, 1093.
[26] E. Kroke, M. Schwarz, *Coordination Chemistry Reviews* **2004**, *248*, 493.
[27] S.-H. Wei, *Comp. Mater. Sci.* **2004**, *30*, 337.
[28] C. G. Van de Walle, J. Neugebauer, *J. Appl. Phys.* **2004**, *95*, 3851.
[29] P. Narang, S. Chen, L.-W. Wang, H. A. Atwater, Unpublished.
[30] S. B. Zhang, S.-H. Wei, A. Zunger, *J. Appl. Phys.* **1998**, *83*, 3192.
[31] E. Fortunato, P. Barquinha, R. Martins, *Adv. Mater.* **2012**, *24*, 2945.
[32] A. Walsh, J. L. F. Da Silva, S.-H. Wei, C. Körber, A. Klein, L. F. J. Piper, A. DeMasi, K. E. Smith, G. Panaccione, P. Torelli, D. J. Payne, A. Bourlange, R. G. Egdell, *Phys. Rev. Lett.* **2008**, *100*, 167402.
[33] A. Kuwabara, *Science and Technology of Advanced Materials* **2007**, *8*, 519.
[34] G. Kresse, J. Furthmueller, *Phys. Rev. B* **1996**, *54*, 11169.
[35] G. Kresse, D. Joubert, *Phys. Rev. B* **1999**, *59*, 1758.
[36] J. Paier, M. Marsman, K. Hummer, G. Kresse, I. C. Gerber, J. G. Ángyán, *J. Chem. Phys.* **2006**, *124*, 154709.
[37] J. L. Lyons, A. Janotti, C. G. Van de Walle, *Appl. Phys. Lett.* **2010**, *97*, 152108.
[38] Q. Yan, A. Janotti, M. Scheffler, C. Van de Walle, *Appl. Phys. Lett.* **2012**, *100*, 142110.